Mars Global Surveyor and Mars Odyssey Accelerometer observations of the Martian upper atmosphere during aerobraking

Paul Withers

Center for Space Physics, Boston University, Boston, Massachusetts, USA

Received 22 August 2005; revised 11 October 2005; accepted 12 November 2005; published 17 January 2006.

[1] Mars Global Surveyor and Mars Odyssey accelerometer measurements of martian upper atmospheric densities reveal the large-scale and small-scale structure of the thermosphere in unprecedented detail. Meridional density gradients, which are seasonally dependent, are greater on the dayside than the nightside, indicating stronger meridional winds on the dayside. Density scale heights do not vary greatly with latitude. Densities and density scale heights are lower on the nightside than on the dayside, but the day-night contrast is not as great as at Venus. Thus atmospheric circulation plays a greater role in determining the state of the thermosphere on Mars than on Venus. Oscillations in density along individual density profiles, probably due to gravity waves, are common and their amplitudes are tens of percent. Step-like changes in density are also observed, but their origin is less clear. Data coverage is extensive enough to permit studies of weather, not just climate. **Citation:** Withers, P. (2006), Mars Global Surveyor and Mars Odyssey Accelerometer observations of the Martian upper atmosphere during aerobraking, *Geophys. Res. Lett.*, *33*, L02201, doi:10.1029/2005GL024447.

1. Introduction

[2] In this paper I present observations of the density, ρ, and density scale height, H_ρ, of the martian atmosphere that were derived from accelerometer (ACC) observations made when Mars Global Surveyor (MGS) and Mars Odyssey (ODY) aerobraked at Mars. My aim is to highlight the rich variety of atmospheric phenomena and processes that can be seen in these observations.

[3] MGS reached Mars in September 1997 and concluded Phase 1 of its aerobraking in March 1998. Phase 2 of aerobraking began in September 1998 and concluded in February 1999. ODY reached Mars in October 2001 and concluded its aerobraking on January 2002. Mars Reconnaissance Orbiter (MRO) will begin aerobraking in March 2006.

[4] The latitude, local solar time (LST), and altitude of periapsis during MGS and ODY aerobraking are shown in Figure 1. Sampling in longitude is excellent. Predicted values of these properties for MRO are also shown in Figure 1. Actual values may differ from those shown. The orbits of MGS and ODY were nearly sun-synchronous and had inclinations of $\sim$93°. Aerobraking passes, except for those near the poles, were meridional. Time series of atmospheric density along the spacecraft's trajectory were derived from accelerometer measurements [*Cancro et al.*, 1998; *Tolson et al.*, 1999, 2000]. MGS and ODY typically flew tens of kilometres horizontally for every kilometre of vertical flight within the atmosphere, so these density profiles are not vertical. Densities and density scale heights at fixed altitudes were extracted from these profiles. MGS density profiles and fixed altitude data sets have been archived at the Planetary Data System (PDS) and peer-reviewed [*Keating et al.*, 2001a, 2001b]. The profiles give 7-second and 40-second averages of density at a sampling rate of 1 Hz. These 7-second and 40-second averaging intervals were chosen during MGS operations. The shorter interval removes the effects of oscillations of a damaged solar panel, whose period was about 7 seconds, and retains significant small-scale structure. The longer interval reduces the spatial resolution of the data, but provides greater vertical range. The fixed altitudes are 130, 140, 150, and 160 km. ODY density profiles are not available from the PDS. ODY fixed altitude data sets (110 and 120 km) are available from the PDS, but have not undergone peer-review since their delivery to the PDS in August 2002 [*Keating et al.*, 2004].

[5] Basic physical processes, radiative transfer and fluid dynamics, control the structure of the martian thermosphere. Heating is caused by the absorption of solar EUV/UV photons and convergence of flow. Cooling is caused by IR radiation and divergence of flow. Understanding the balances between heating and cooling and between radiative processes and dynamical processes is essential for a full understanding of the martian thermosphere.

[6] Most previous work on the MGS ACC data set has concerned zonal density variations caused by thermal tides [*Joshi et al.*, 2000; *Forbes and Hagan*, 2000; *Forbes et al.*, 2002; *Wilson*, 2002; *Withers*, 2003; *Withers et al.*, 2003; *Angelats i Coll et al.*, 2004]. Workers have also used the data sets for general investigations [*Keating et al.*, 1998; *Bougher et al.*, 1999] and as context for ionospheric studies [*Bougher et al.*, 2001, 2004; *Breus et al.*, 2004; *Krymskii et al.*, 2004]. There have been few publications concerning the ODY ACC data set [*Krymskii et al.*, 2003; *Tolson et al.*, 2005; S. W. Bougher et al. (2005), Polar warming in the Mars lower thermosphere: Seasonal variations owing to changing solar insolation and dust distributions, submitted to *Geophysical Research Letters*, 2005, hereinafter referred to as Bougher et al., submitted manuscript, 2005].

2. Observations

[7] I begin with studies of the fixed altitude ρ and H_ρ observations. I have derived values of ρ and H_ρ at 120 km from the MGS density profiles in order to make comparisons between MGS and ODY observations. Discarding

0094-8276/06/2005GL024447$05.00

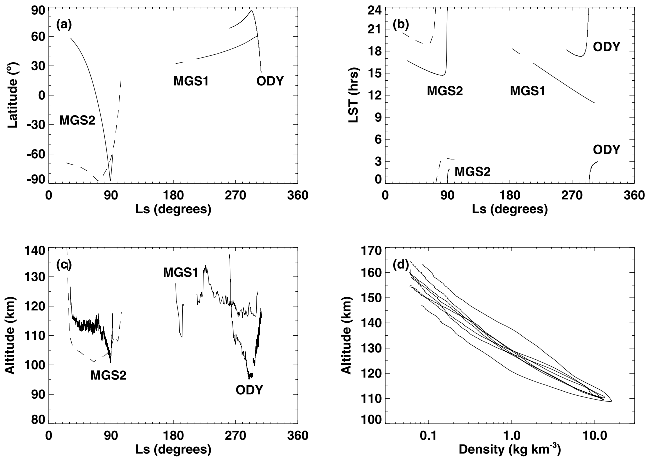

Figure 1. Panels (a), (b), and (c): Periapsis latitude, LST, and altitude for MGS Phase 1, MGS Phase 2, and ODY aerobraking (solid lines). Predicted values of these properties for MRO aerobraking are shown by the dashed lines. MGS Phase 1 aerobraking was interrupted around Ls = 200° by a dust storm. Panel (d): 40-second density profiles for MGS orbits P0963 (periapsis at 24°S, 138°E, 31 December 1998), P0970 (26°S, 130°E, 1 January 1999), P0977 (28°S, 128°E, 2 January 1999), and P0984 (29°S, 133°E, 3 January 1999). The P977 density profile is clearly distinct from the other three. Measurement uncertainties at 120 km are less than 0.2 kg km^{-3}.

observations poleward of 80° latitude, I classify the fixed altitude MGS and ODY data into five groups based partially on their LST: MGS Phase 1, MGS Phase 2/pm, MGS Phase 2/am, ODY/pm, and ODY/am.

[8] Panel (a) of Figure 2 shows inbound and outbound MGS and ODY measurements of ρ at 120 km. Sampling in longitude is complete and unbiased within each latitude bin shown in Figure 2. Inbound and outbound observations, typically separated in time by a few weeks, are quite similar to each other. With the exception of MGS Phase 1, the changes in ρ shown in this panel should primarily be due to changes in latitude because changes in LST and Ls are fairly small within each of the four remaining subsets. Meridional density gradients are greater on the dayside than on the nightside, so meridional flow is stronger on the dayside than the nightside. Seasonal reversals in the dayside meridional density gradient correspond to seasonal reversals in the dayside meridional flow direction. Panel (b) of Figure 2 shows the corresponding values of H_ρ, which are smaller at night than during the day. Periapsis altitude in MGS Phase 1 was often barely below 120 km, so occasional large values of H_ρ in this subset of observations are probably due to the effects of horizontal gradients.

[9] The pressure scale height, H, is related to temperature, T, by $\mu g H = kT$, where μ is the mean molecular mass, g is the acceleration due to gravity, and k is Boltzmann's constant. An estimate of the temperature, T_ρ, can be obtained from the density scale height, H_ρ, using $\mu g H_\rho = kT_\rho$. I use $g = 3.47$ m s^{-2} and $\mu = 43.49$ daltons [*Magalhães et al.*, 1999]. In an isothermal atmosphere with uniform mean molecular mass, $H_\rho = H$. Panel (c) of Figure 2 shows values of T_ρ corresponding to the data in Panels (a) and (b) of Figure 2. Temperatures are coldest on the nightside, indicating that direct solar heating plays an important role in controlling the thermal structure of the thermosphere, but the nightside temperatures are not much colder than the dayside. On Venus, the nightside temperatures are much lower than those of the dayside due to its long solar day. Additional mechanisms, such as turbulence-induced friction from gravity wave drag, are also required on Venus to restrict the expected strong sub-solar to anti-solar circulation and reduce the nightside dynamical heating and temperatures [*Bougher et al.*, 2002]. Despite similarities in one fundamental parameter, chemical composition, and subsequently similar radiative processes, differences in another fundamental parameter, rotation rate, and subsequently different circulation patterns cause the thermospheres of Venus and Mars to have significantly different diurnal cycles. Temperatures in the northern polar regions increase toward the pole, whereas temperatures at other latitudes, including the southern polar region, are quite insensitive to latitude (Bougher et al., submitted manuscript, 2005).

[10] Panel (d) of Figure 2 shows inbound and outbound densities at 120, 130, 140, 150, and 160 km versus latitude from MGS Phase 2/pm. The corresponding values of H_ρ and T_ρ are shown in Panels (e) and (f) of Figure 2. It is striking that temperature varies much more over 40 km of altitude

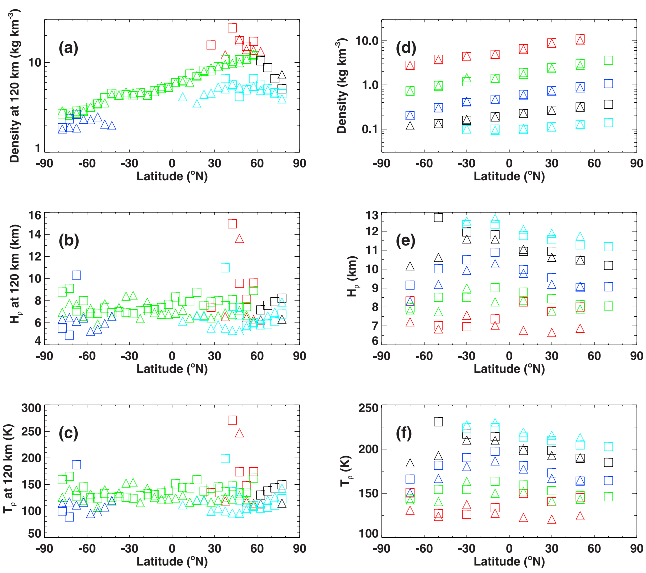

Figure 2. Panel (a): Density at 120 km versus latitude. Mean densities for 5° latitude bins are plotted. Triangles indicate inbound observations, squares indicate outbound observations. Red symbols indicate MGS Phase 1, green indicates MGS Phase 2/pm, dark blue indicates MGS Phase 2/am, black indicates ODY/pm, and light blue indicates ODY/am. Panel (b): As Panel (a), but showing density scale height, H_ρ. Panel (c): As Panel (a), but showing estimated temperature, T_ρ. Panel (d): Density at 120, 130, 140, 150, and 160 km from MGS Phase 2/pm. Mean densities for 20° latitude bins are plotted. Triangles indicate inbound observations, squares indicate outbound observations. Red symbols indicate 120 km, green indicates 130 km, dark blue indicates 140 km, black indicates 150 km, and light blue indicates 160 km. Panel (e): As Panel (d), but showing density scale height, H_ρ. Panel (f): As Panel (d), but showing estimated temperature, T_ρ.

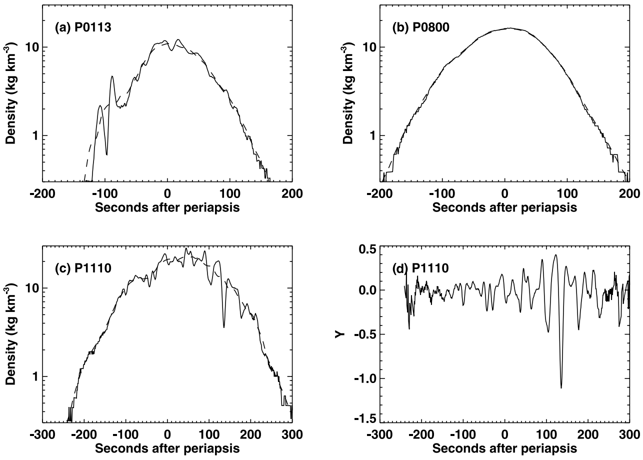

Figure 3. Panels (a), (b), and (c): Density profiles from MGS orbits P0113, P0800, and P1110. 7-second densities are marked by solid lines, 40-second densities by dashed lines. Panel (d): Y versus time for MGS orbit P1110. The strongest oscillations occur at 140 km in orbit P0113 and 110 km in orbit P1110.

than it does over 80° of latitude. Atmospheric circulation transports heat horizontally away from the sub-solar point effectively, but the large vertical temperature gradient is maintained by thermal conduction. Heat produced at high altitudes by the absorption of solar EUV/UV photons is conducted downward toward the mesopause where it can be lost by IR radiation [*Bougher et al.*, 2002]. The effects of atmospheric circulation have shifted the latitude of maximum temperatures away from the sub-solar point in the northern tropics to the southern tropics, which is consistent with the strong and vertically-extended inter-hemispheric circulation that is known to occur on Mars at this season [*Zurek et al.*, 1992; *Bougher et al.*, 2000, also submitted manuscript, 2005].

[11] I now turn to studies of 7-second and 40-second density profiles. These profiles, especially the 7-second density profiles, contain small-scale structure that is not present in the fixed-altitude data products. Panels (a), (b), and (c) of Figure 3 show oscillatory small-scale structure. The amplitude, typically tens of percent, and observed period, typically tens of seconds, of these oscillations can vary within a given profile and between different profiles. The 7-second and 40-second densities can differ by a factor of two. This type of small-scale structure is probably due to gravity waves [*Bougher et al.*, 1999; *Tolson et al.*, 1999, 2005]. The degree to which small-scale structure is present in a given aerobraking pass can be quantified by the following figure-of-merit, X:

$$Y = 2\frac{(\rho_7 - \rho_{40})}{(\rho_7 + \rho_{40})} \tag{1}$$

$$X = \sqrt{\overline{Y^2}} \tag{2}$$

where ρ_7 and ρ_{40} are 7-second and 40-second densities, respectively, and $\overline{Y^2}$ is the mean value of Y^2. Panel (a) of Figure 4 shows X versus latitude. All the data shown here are consistent with low values of X in the tropics and high values of X, meaning extensive small-scale structure, in regions on the order of 30° wide centred on 60°N and 60°S. Although the Noachis regional dust storm occurred during MGS Phase 1, it dissipated before the end of MGS Phase 1 and so cannot be solely responsible for the large values of X during this period. X will be affected by the conditions under which gravity waves are excited in the lower atmosphere and propagate upward.

[12] Not all small-scale structures have oscillatory shapes. The examples in Panels (b), (c), and (d) of Figure 4 show sudden changes in density that appear more step-like than oscillatory. It is possible that these phenomena are associated with inadequate removal of spacecraft oscillations due to MGS's damaged solar panel, but their cause, whether atmospheric or spacecraft-related, has not been identified convincingly. Searches for similar phenomena in the ODY density profiles will be valuable [*Tolson et al.*, 1999, 2005].

[13] As discussed by *Withers et al.* [2003], the same latitudes, longitudes, and altitudes were occasionally sampled by repeated aerobraking passes at the same LST and Ls on consecutive sols, or martian days, during "resonances" between MGS's orbital period and the martian rotational period. Panel (d) of Figure 1 shows four such density profiles. Three of them are very similar, but one is clearly distinct. Studies of weather, not climate, in the martian thermosphere will be necessary to interpret such observations.

3. Conclusions

[14] The thermospheres of the three terrestrial planets are natural laboratories within which the same basic physical processes, such as fluid dynamics, radiative transfer, and photochemistry, operate. Differences in atmospheric composition, magnetic field, rotational rate, gravity, distance from the Sun, and obliquity cause differences between conditions in the three thermospheres [*Bougher et al.*,

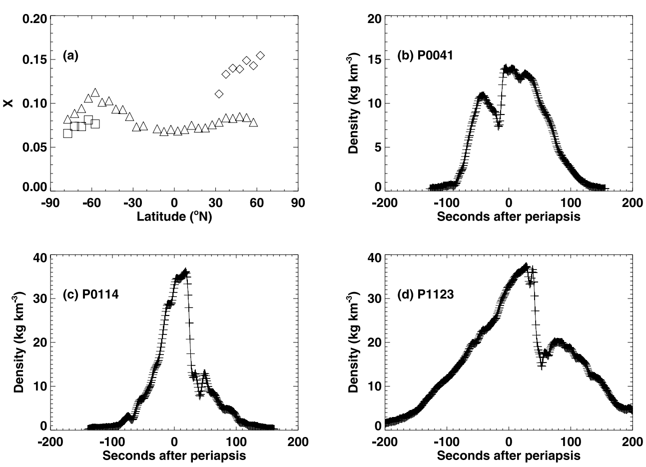

Figure 4. Panel (a): Measure of small-scale structure, X, for MGS Phase 1 (diamonds), MGS Phase 2/pm (triangles), and MGS Phase 2/am (squares). Mean values for 5° latitude bins are plotted. Panels (b), (c), and (d): Profiles of 7-second density from MGS orbits P0041, P0114, and P1123. Each of the measurements, which are separated by 1 second, is marked by a cross.

2002]. Due to a relative lack of observations, the martian thermosphere is currently the least understood of these three. Indeed, many theories concerning the martian thermosphere are based heavily on analogy to Venus. The observations presented here will test those theories, thereby highlighting significant differences between the thermospheres of Venus and Mars, and improving our understanding of the relevant physical processes.

[15] The observations presented here shed new light on the balances between heating and cooling and between radiative processes and dynamical processes in the martian thermosphere. These are some of the first observations of the nightside thermosphere of Mars and show that, unlike Venus, it is not much colder than the dayside.

[16] The Mars Express ASPERA instrument has observed ions and neutrals escaping from the martian atmosphere. Knowledge of upper atmospheric conditions, such as the observations in this paper, is needed if the ASPERA observations are to be used to improve models of volatile loss through escape. Synthesis of lower (MGS TES), middle (Mars Express SPICAM and MRO Mars Climate Sounder), and upper atmospheric data sets (MGS, ODY, and MRO ACC) into an integrated picture of the circulation and thermal structure of the whole martian atmosphere will provide the observational foundations for addressing important theoretical questions concerning many aspects of both martian science and atmospheric science.

[17] **Acknowledgments.** I acknowledge support from the NSF CEDAR postdoctoral program and the NASA Mars Data Analysis Program. I acknowledge helpful reviews by Steve Bougher and an anonymous referee.

References

Angelats i Coll, M., F. Forget, M. A. López-Valverde, P. L. Read, and S. R. Lewis (2004), Upper atmosphere of Mars up to 120 km: Mars Global Surveyor accelerometer data analysis with the LMD general circulation model, *J. Geophys. Res.*, *109*, E01011, doi:10.1029/2003JE002163.

Bougher, S., G. Keating, R. Zurek, J. Murphy, R. Haberle, J. Hollingsworth, and R. T. Clancy (1999), Mars Global Surveyor aerobraking: Atmospheric trends and model interpretation, *Adv. Space Res.*, *23*, 1887–1897.

Bougher, S. W., S. Engel, R. G. Roble, and B. Foster (2000), Comparative terrestrial planet thermospheres: 3. Solar cycle variation of global structure and winds at solstices, *J. Geophys. Res.*, *105*(E7), 17,669–17,692.

Bougher, S. W., S. Engel, D. P. Hinson, and J. M. Forbes (2001), Mars Global Surveyor Radio Science electron density profiles: Neutral atmosphere implications, *Geophys. Res. Lett.*, *28*, 3091–3094.

Bougher, S. W., R. G. Roble, and T. Fuller-Rowell (2002), Simulations of the upper atmospheres of the terrestrial planets, in *Atmospheres in the Solar System: Comparative Aeronomy*, *Geophys. Monogr. Ser.*, vol. 130, edited by M. Mendillo, A. F. Nagy, and J. H. Waite, pp. 261–288, AGU, Washington, D. C.

Bougher, S. W., S. Engel, D. P. Hinson, and J. R. Murphy (2004), MGS Radio Science electron density profiles: Interannual variability and implications for the Martian neutral atmosphere, *J. Geophys. Res.*, *109*, E03010, doi:10.1029/2003JE002154.

Breus, T. K., A. M. Krymskii, D. H. Crider, N. F. Ness, D. Hinson, and K. K. Barashyan (2004), Effect of the solar radiation in the topside atmosphere/ionosphere of Mars: Mars Global Surveyor observations, *J. Geophys. Res.*, *109*, A09310, doi:10.1029/2004JA010431.

Cancro, G. J., G. M. Keating, and R. H. Tolson (1998), Operational data reduction procedure for determining density and vertical structure of the Martian upper atmosphere from Mars Global Surveyor Accelerometer measurements, also NASA/CR-998-208721, Master's thesis, Joint Inst. for Adv. Flight Stud., George Washington Univ. and NASA Langley Res. Cent., Hampton, Va.

Forbes, J. M., and M. E. Hagan (2000), Diurnal Kelvin wave in the atmosphere of Mars: Towards an understanding of "stationary" density structures observed by the MGS accelerometer, *Geophys. Res. Lett.*, *27*, 3563–3566.

Forbes, J. M., A. F. C. Bridger, S. W. Bougher, M. E. Hagan, J. L. Hollingsworth, G. M. Keating, and J. Murphy (2002), Nonmigrating tides in the thermosphere of Mars, *J. Geophys. Res.*, *107*(E11), 5113, doi:10.1029/2001JE001582.

Joshi, M. M., J. L. Hollingsworth, R. M. Haberle, and A. F. C. Bridger (2000), An interpretation of Martian thermospheric waves based on analysis of a general circulation model, *Geophys. Res. Lett.*, *27*, 613–616.

Keating, G. M., et al. (1998), The structure of the upper atmosphere of Mars: In situ accelerometer measurements from Mars Global Surveyor, *Science*, *279*, 1672–1676.

Keating, G. M., R. H. Tolson, J. L. Hanna, R. F. Beebe, J. R. Murphy, and L. Huber (2001a), MGS-M-ACCEL-5-ALTITUDE-V1.1, http://atmos.nmsu.edu/PDS/data/mgsa_0002/, NASA Planet. Data Syst., NASA Goddard Space Flight Cent., Greenbelt, Md.

Keating, G. M., R. H. Tolson, J. L. Hanna, R. F. Beebe, J. R. Murphy, and L. Huber (2001b), MGS-M-ACCEL-5-PROFILE-V1.1, http://atmos.nmsu.edu/PDS/data/mgsa_0002/, NASA Planet. Data Syst., NASA Goddard Space Flight Cent., Greenbelt, Md.

Keating, G. M., J. R. Murphy, R. F. Beebe, and L. Huber (2004), ODY-M-ACCEL-5-ALTITUDE-V1.0, http://pds-atmospheres.nmsu.edu/data_and_services/atmospheres_data/odyacc.html, NASA Planet. Data Syst., NASA Goddard Space Flight Cent., Greenbelt, Md.

Krymskii, A. M., T. K. Breus, N. F. Ness, D. P. Hinson, and D. I. Bojkov (2003), Effect of crustal magnetic fields on the near terminator ionosphere at Mars: Comparison of in situ magnetic field measurements with the data of radio science experiments on board Mars Global Surveyor, *J. Geophys. Res.*, *108*(A12), 1431, doi:10.1029/2002JA009662.

Krymskii, A. M., N. F. Ness, D. H. Crider, T. K. Breus, M. H. Acuña, and D. P. Hinson (2004), Solar wind interaction with the ionosphere/atmosphere and crustal magnetic fields at Mars: Mars Global Surveyor Magnetometer/Electron Reflectometer, radio science, and accelerometer data, *J. Geophys. Res.*, *109*, A11306, doi:10.1029/2004JA010420.

Magalhães, J. A., J. T. Schofield, and A. Seiff (1999), Results of the Mars Pathfinder atmospheric structure investigation, *J. Geophys. Res.*, *104*(E4), 8943–8956.

Tolson, R. H., G. M. Keating, G. J. Cancro, J. S. Parker, S. N. Noll, and B. L. Wilkerson (1999), Application of accelerometer data to Mars Global Surveyor aerobraking operations, *J. Spacecr. Rockets*, *36*, 323–329.

Tolson, R. H., G. M. Keating, S. N. Noll, D. T. Baird, and T. J. Shellenberg (2000), Utilization of Mars Global Surveyor accelerometer data for atmospheric modeling, *Adv. Astronaut. Sci.*, *103*, 1329–1346.

Tolson, R. H., A. M. Dwyer, J. L. Hanna, G. M. Keating, B. E. George, P. E. Escalera, and M. R. Werner (2005), Application of accelerometer data to Mars Odyssey aerobraking and atmospheric modeling, *J. Spacecr. Rockets*, *42*, 435–443.

Wilson, R. J. (2002), Evidence for nonmigrating thermal tides in the Mars upper atmosphere from the Mars Global Surveyor accelerometer experiment, *Geophys. Res. Lett.*, *29*(7), 1120, doi:10.1029/2001GL013975.

Withers, P. (2003), Tides in the Martian atmosphere and other topics, Ph.D. thesis, Univ. of Ariz., Tucson.

Withers, P., S. W. Bougher, and G. M. Keating (2003), The effects of topographically-controlled thermal tides in the Martian upper atmosphere as seen by the MGS accelerometer, *Icarus*, *164*, 14–32.

Zurek, R. W., J. R. Barnes, R. M. Haberle, J. B. Pollack, J. E. Tillman, and C. B. Leovy (1992), Dynamics of the atmosphere of Mars, in *Mars*, edited by H. H. Kieffer et al., pp. 835–933, Univ. of Ariz. Press, Tucson.

P. Withers, Center for Space Physics, Boston University, 725 Commonwealth Avenue, Boston MA 02215, USA. (withers@bu.edu)